

Radiation emitted by channeled positrons in the continuous potential of the planes of a crystal

V. A. Bazylev, V. V. Beloshitskiĭ, V. I. Glebov, N. K. Zhevago, M. A. Kumakhov, and Kh. Trikalinos

I. V. Kurchatov Institute of Atomic Energy

(Submitted 12 March 1980; resubmitted 26 September 1980)

Zh. Eksp. Teor. Fiz. **80**, 608–626 (February 1981)

The characteristics, measured recently in a Soviet-American experiment, of the radiation emitted by channeled positrons are compared with the results of theoretical calculations. It is shown that the experimental data can be explained by the effect, theoretically predicted earlier by Kumakhov, of spontaneous emission by channeled particles.

PACS numbers: 61.80.Mk

The possibility of intense x - and γ -ray emission by channeling particles moving in the continuous potential planes and axes of a crystal was first predicted by Kumakhov.¹ The theory of this phenomenon was subsequently developed by us and others in a number of papers.²⁻⁸ In particular, the characteristics of the radiation emitted by particles of relatively high energies ($\geq 1-10$ GeV) are considered in Refs. 4 and 6-8.

In the present paper we carry out a detailed analysis of the theoretical results, and compare them with the available experimental data⁹ on the spectra of the radiation emitted by positrons with energies of several GeV in the case of planar channeling.

1. THEORY OF THE EMISSION IN THE CASE OF PLANAR CHANNELING

The spectral-angular distribution of the radiation intensity in the case of planar channeling is derived in its most general form in Ref. 6. This distribution has the form¹⁾ [see the formulas (10)-(12) in Ref. 6]

$$\frac{d^2W}{d\omega d\Omega} = \frac{e^2\omega^2}{2\pi} \sum_f \left\{ \left(1+u + \frac{u^2}{2} \right) [|I_{if}^{(1)}|^2 \theta^2 + |I_{if}^{(2)}|^2 - 2 \operatorname{Re} I_{if}^{(1)} I_{if}^{(2)*} \theta \cos \varphi] + \frac{u^2}{2E^2} |I_{if}^{(1)}|^2 \right\} \delta \left[\frac{u}{2} ((\theta^2 + E^{-2})E - \omega \theta^2 \cos^2 \varphi) - \omega_{if} \right]. \quad (1)$$

Here E is the initial particle energy; $\omega_{if} = \varepsilon_i(E) - \varepsilon_f(E - \omega)$ is the difference between the transverse-motion energies $I_{if}^{(1,2)}$ are the matrix elements of the current associated with the transition between the transverse-energy levels [see (7) in Ref. 6]; ω is the photon energy; $u = \omega/(E - \omega)$; θ and φ are the polar and azimuthal emission angles; $d\Omega = \theta d\theta d\varphi$; and δ is a generalized Dirac function.

In deriving the expression (1), allowance is made for 1) the possibility that the radiative transitions have a non-dipole character, 2) the parametric coupling of the transverse and longitudinal motions, a coupling which manifests itself in the dependence of the energy levels and the wave functions of the transverse motion on the total energy E , 3) the influence of the quantum efficiency on the longitudinal and transverse motions, and 4) the interaction of the positron (electron) spin with the radiation field. The expression (1) is derived under the condition that the channeled particle's transverse energy is small compared to its total energy. It is also

assumed that the particle is ultrarelativistic, and that the effective-emission polar angles are small. These conditions are almost always fulfilled.

The presence of the δ function is a consequence of the laws of conservation of the energy and of the longitudinal component of the momentum during the emission:

$$\varepsilon_i(E_i) + E_i'' - \varepsilon_f(E_f) - E_f'' = \omega, \quad \mathbf{p}_i'' - \mathbf{p}_f'' = \mathbf{k}'', \quad (2)$$

where $E'' = (1 + p''^2)^{1/2}$ is the energy of the longitudinal motion of the channeled particle, $\varepsilon_i(E_i)$ and $\varepsilon_f(E_f)$ are the quantized energies of the transverse motion, which parametrically depend on the particle's relativistic mass E . The dependence of the energy of the emitted photon on the direction of emission is thereby fixed. Notice that the energy of a fairly hard photon ($\omega \sim E$) depends on both the polar, θ , and the azimuthal, φ , angles of emission.²⁾

For transitions between transverse-energy levels with fixed quantum numbers i and f , the photon has its maximum energy ω_m when it is emitted at the angle $\theta = 0$. In this case its energy is given by the equation

$$\omega_m/2E(E - \omega_m) = \varepsilon_i(E) - \varepsilon_f(E - \omega_m). \quad (3)$$

The absolute upper limit, ω_{am} , of the spectrum corresponds to a transition to the bottom of the potential well, when $\varepsilon_f \approx 0$:

$$\omega_{am}/E = 2\varepsilon_i E / (1 + 2\varepsilon_i E). \quad (4)$$

From this relation it follows firstly, that relatively hard photons with $\omega \sim E$ can be emitted only by particles with a fairly high energy $E \geq (mc^2)^2/\varepsilon_i$, which corresponds to several GeV for planar channeling. Secondly, hard ($\omega \sim E$) photons can be emitted only in transitions involving relatively large ($i - f \sim i$) quantum-number changes, when the difference between the transverse energies is comparable to the energies themselves ($\omega_{if} \sim \varepsilon_i$).

The matrix elements of the current associated with a transition can be computed analytically for a number of model planar potentials. For a parabolic potential, $U(x) = 4U_0 x^2/d^2$, they have the form^{6,7}

$$I_{if}^{(1)} = \sum_{j'} C_{j'f} J_{if}^{(1)}, \quad I_{if}^{(2)} = \sum_{j'} \left(\frac{\tilde{\omega}_{if}}{k_x} + \frac{k_x}{2E} \right) C_{j'f} J_{if}^{(2)}, \quad (5)$$

where

$$J_{ij}^{(1)} = \left(\frac{i_{<}}{i_{>}} \right)^{1/2} (-2\xi)^{(i_{>}-i_{<})} e^{-\xi} L_{i_{>}}^{i_{<}} (2\xi) (\text{sign } k_x)^{i_{>}-i_{<}}, \quad (6)$$

$$C_{ff'} = \begin{cases} (f_{<}/f_{>})^{1/2} x^{i_{>}} P_{(f_{>}-f_{<})/2}^{(f_{>}+f_{<})/2}(x), & f-f' \text{ even} \\ 0 & f-f' \text{ odd} \end{cases}$$

$$i_{>} = \max\{i, f'\}, \quad f_{>} = \max\{f, f'\}$$

$$i_{<} = \min\{i, f'\}, \quad f_{<} = \min\{f, f'\}$$

$$\xi = \frac{k_x^2 d}{2^{1/2} (U_0 E)^{1/2}}, \quad x = \frac{2E^{-1/2} (E-\omega)^{-1/2}}{E^{-1/2} + (E-\omega)^{-1/2}}$$

L_q^p is a Laguerre polynomial,¹⁰ $P_r^t(x)$ is a Legendre function.¹⁰ Since r and t are whole numbers, the latter is also a polynomial of degree $f_{>}$ in x (see Ref. 10, Sec. 3.6.1).

The level energies of the transverse motion are quantized according to the equations

$$\varepsilon_i(E) = \frac{2}{d} \left(\frac{2U_0}{E} \right)^{1/2} \left(i + \frac{1}{2} \right), \quad \varepsilon_f(E-\omega) = \varepsilon_f(E) \left(\frac{E}{E-\omega} \right)^{1/2}$$

The solution to Eq. (3) in the case of a parabolic potential has the form

$$\omega_m = \frac{2E^2}{1+2\varepsilon_i E} \left(\varepsilon_i - \bar{\varepsilon}_i \frac{\varepsilon_i E + [1+2\varepsilon_i E + \bar{\varepsilon}_i^2 E^2]^{1/2}}{1+2\varepsilon_i E} \right), \quad (7)$$

$$\bar{\varepsilon}_i = \varepsilon_f(E), \quad \varepsilon_i = \varepsilon_i(E)$$

The matrix elements of the current associated with a transition can be represented in an analytical form also for a model planar potential of the type of the Peschel-Teller potential $U(x) = -U_0 \cosh^{-2}(x/b)$ [see the formula (16) in Ref. 7].

Since our main purpose in the present paper is to analyze the emission spectra of high-energy positrons, we shall thoroughly investigate the expressions (5) and (6), which pertain to a parabolic potential. The point is that, for positrons, such a model potential turns out in the majority of cases to be close in form to the more exact potential of the planar channel (see Sec. 4 below).

The obtained expressions, (5) and (6) can be simplified to various degrees in a number of limiting cases. In particular, the following representation of the Legendre functions with arguments close to unity.

$$P_{(f+f')/2}^{(f-f')/2}(x) \approx \left(\frac{f+f'+1}{2} \right)^{1/2} J_{-|f-f'|/2}(\beta), \quad (8)$$

where $J_{-m}(\beta)$ is a Bessel function and $\beta = (\omega/8E)(f+f'+1)$ is valid in the region of relatively soft ($\omega \ll E$) photons [see the formulas (3), (5), and (10) in Ref. 10]. If the parameter $\beta < \frac{1}{4}$, a condition which is fulfilled at energies $E < (mc^2)^2/U_0$, then it can be assumed with sufficient accuracy that³⁾

$$C_{ff'} \approx \delta_{ff'}, \quad (9)$$

where $\delta_{ff'}$ is the Kronecker symbol. Then the general formula (1) reduces to the simpler form obtained in Refs. 4 and 5. In this limiting case the effect of the parametric coupling of the longitudinal and transverse motions on the interlevel transitions is neglected. Such an analysis can be carried out only for lower particle energies, when the stronger inequality $E \ll (mc^2)^2/U_0$ is fulfilled. The effective values of the parameter ξ in (6) then turn out to be small, and, besides (9), the approximate equality

$$J_{ij}^{(1)} \approx \sqrt{-1} k_x (f'/2E\bar{\omega}_0)^{1/2} \delta_{i,f'+1}; \quad \bar{\omega}_0 = d^{-1} (8U_0/E)^{1/2} \quad (10)$$

is valid. In this limit only the dipole transition to the transverse-energy level nearest to the initial level turns out to be important. It is precisely this case that was considered by Kumakhov in his first papers.^{1,2} Under conditions of the dipole approximation, it is relatively easy to allow for the effect of anharmonic corrections to the potential on the spectral distribution of the radiation.^{3,11}

The expressions (6) can be simplified without assuming the condition $\omega \ll E$. This is due to the fact that, at sufficiently high energies, when the emission of photons with energy $\omega \sim E$ becomes possible [see (4)], the number of levels in the potential well for the transverse motion attains values ~ 100 for positrons and several scores for electrons. Therefore, if we do not consider the transitions to the lowest levels, i.e., to the levels with relatively small quantum numbers f , then the wave functions of both the initial and final states have a quasi-classical character. Then we can use the asymptotic representations of the polynomials L_n^μ and functions P_{nm} for large values of the indices ν and n [see the formulas (10), (15), and (2) in Ref. 10]. As a result, we obtain

$$J_{ij}^{(1)} \approx (-1)^{(i_{>}-i_{<})/2} \left(\frac{i_{>}}{i_{<}} \right)^{1/2} \left(\frac{\nu}{4} \right)^{(i_{>}-i_{<})/2} J_{i_{>}-i_{<}}(n_x a_0 \nu^{1/2}),$$

$$C_{ff'} = \left(\frac{f_{<}}{f_{>}} \right)^{1/2} \frac{2^{-|f-f'|/4}}{[(f+f')/2+1]^{-|f-f'|/2}} \frac{x^{1/2}}{(1+x)^{-|f-f'|/4}} J_{-|f-f'|/2}(x) \quad (11)$$

for even values of the difference $f-f'$; $C_{ff'} = 0$ if $f-f'$ is odd. Further:

$$\nu = 6i_{>} - 2i_{<} - 2, \quad a_0 = d^{1/2} / 2^{1/2} (U_0 E)^{1/2},$$

$$x = [(f+f')/2+1][2(1-x)]^{1/2}$$

For the factorials in (11) we can use here Stirling's asymptotic representation [see the formulas (1), (18), and (3) in Ref. 10].

If moreover the differences between the quantum numbers of the levels between which the transition occurs are significantly smaller than the numbers themselves, i.e., if $|f-f'| \ll f$ and $|i-f| \ll i$, then further simplifications of the quantities (11) are possible. As has already been noted above, in transitions to the nearest ($i-f \ll i$) levels channeled particles always emit photons with relatively low energies $\omega \ll E$. Therefore, the limiting case under consideration corresponds to a transition to the classical description of both the particle motion and the emission process. After further simplifications of the quantities (11), we obtain

$$C_{ff'} J_{ij}^{(1)} \approx (-1)^{n/2} J_{n+2m}(k_x a) J_m(\beta), \quad (12)$$

where $a = 2a_0(\varepsilon/\omega_0)^{1/2}$, $\beta = \omega\varepsilon/4E\omega_0$, $n = i-f$, and $m = (f-f')/2$. At the same time, taking account of the condition $\omega \ll E$, we can, in computing the argument of the δ function in (1), use the approximate equality

$$\varepsilon_f(E-\omega) \approx \varepsilon_f(E) - \omega \partial \varepsilon_f / \partial E, \quad (13)$$

where $\partial \varepsilon / \partial E = -\varepsilon/2E$ for a parabolic potential. Furthermore, the dependence of the photon energy on the azimuthal angle becomes unimportant for relatively soft ($\omega \ll E$) photons [see (1)]. These results are also ob-

tained if from the very beginning we replace in the expression (1) the matrix elements of the current by the Fourier transforms of the corresponding classical quantities [see (19) in Ref. 7], and compute them for a parabolic potential. The computations are similar to those carried out in, for example, investigations of the emission in undulators with a harmonic transverse field.^{12,13}

2. COMPARISON WITH THE RESULTS OF OTHER AUTHORS

A paper¹⁴ devoted to the study of radiation emission by channeled particles has recently been published by Baier *et al.* A formula, (5.3), is derived in this paper for the spectral-angular distribution of the intensity with allowance for the quantum effects involved in radiation emission. This formula essentially differs from the results, (1) and (11), used in the present paper. According to Baier *et al.*,¹⁴ the radiation frequency does not depend on the azimuthal angle even when the quantum efficiency is taken into account. This contradicts the conservation laws (2), which lead to a dependence of the radiation frequency of a fairly hard photon on the azimuthal angle φ .

The most important error of Baier *et al.*¹⁴ is that they use in the radiation computations for channeled particles the results obtained for radiation emission in undulators with a transverse field. The vibration frequency of particles in a channel, unlike in undulators, depends essentially on the total particle energy.¹⁻⁸ Therefore, in the case of channeling, the effect of the emission of a fairly hard ($\omega \sim E$) photon on the transverse motion is quite substantial,⁹ since the total particle energy changes appreciably in the photon-emission process. This effect was not taken into account by Baier *et al.*,¹⁴ and their results are therefore incorrect, at least in the region $\omega \sim E$. It should also be noted that the general approach used by Baier *et al.*¹⁴ to solve the problem of radiation emission by channeled particles takes account of only the quantum character of the radiation, neglecting the quantum character of the particle motion in the channel. This approach is, generally speaking, inadequate for the computation of the radiation emitted by channeled particles, since the emission of a fairly hard ($\omega \sim E$) photon is, as shown above [see (4) and the corresponding text], possible only in transitions involving a relatively large ($i - f \sim i$) change in the quantum numbers of the transverse motion. As a consequence, the matrix elements of the current associated with a transition cannot, when the quantum efficiency is taken into consideration, be expressed in terms of the corresponding classical quantities [see (11)].

On the other hand, the criticisms leveled by Baier *et al.*¹⁴ at the results of the existing theory of emission by channeled particles do not in the majority of cases seem to us to be justified. Thus, the principal formula of Zhevago's paper⁶ [see (1)] is valid for any form of the potential, and not only when $C_{ff'} \sim \delta_{ff'}$, as erroneously asserted in Ref. 14. The maximum radiation frequency for a given transition $i \rightarrow f$ in the case $\varepsilon_i E \gg 1$

is, according to (7), proportional to $E^{1/2}$. The estimate $\omega_m \sim E^2$, given by Baier *et al.*¹⁴ does not, unlike the relation $\omega_m \sim E^{1/2}$, conform with the conservation laws (2), nor with the experimental data (see below).

The emission of hard photons with energy $\hbar\omega \sim E$ in the case of planar channeling has also been recently considered by Baryshevskii *et al.*,¹⁵ whose earlier papers^{16,17} are based on a wrong approach, involving the use of an incorrect asymptotic form of the wave functions of the channeled particles. A detailed review of these papers is contained in Refs. 7, 8 and 18. In spite of this Baryshevskii *et al.* assert in Ref. 15 (see the beginning of Sec. 3) that the procedure employed and their earlier results remain valid without any changes. This assertion is contradictory, since, in the first place, the results of all the three papers¹⁵⁻¹⁷ do not agree among themselves. For example, the general expressions (3) and (6) obtained in Ref. 15 for the particle current $W_{\gamma n}$ contain, in contrast to the analogous expressions (15) of Ref. 16 also the longitudinal component of the current $j_{\gamma n}$, and, in contrast to (3) in Ref. 17 and (15) in Ref. 16, the integrands for the current components [see (3) in Ref. 15] contain the photon wave function $e^{-ik_x x}$. Such discrepancies significantly affect the spectral, angular, and polarization properties of the radiation, but they are ignored without justification by Baryshevskii and his co-workers.¹⁵⁻¹⁷ Secondly, such important characteristics as the emission-angle and particle-energy dependences of the emitted-photon energy are incorrectly determined in Ref. 15 on the basis of this approach. In the limit of sufficiently thick crystals these dependences are determined by setting the right-hand side of the expression (7) in Ref. 15 to zero:

$$\frac{\omega}{2(E-\omega)} \left[(1-n(\omega)\cos\theta)2(E-\omega) + \frac{1}{E} + \omega\theta^2 \sin\varphi - \omega_{if} + 2\varepsilon_i \right] = \omega_{if}. \quad (14)$$

For small θ and a refractive index $n(\omega) = 1$ our calculations yield another result:

$$\frac{1}{2} \omega \left[\theta^2 + \frac{E^{-1} + \omega\theta^2 \sin^2\varphi}{E-\omega} \right] = \omega_{if}. \quad (15)$$

Thus, in comparison with (15), the square brackets in (14) contain two additional terms (the last two terms), which can play quite an important role.¹⁵ Let us know that their presence in (14) contradicts the Doppler relation. Indeed, let us consider the classical limit of the relations (14) and (15). In this limit $\omega \ll E$, $i \gg 1$, and $i - f \ll i$. Therefore, the approximate equality

$$\omega_{if} \approx \tilde{\omega}_{if}(E) + \omega \partial \varepsilon_i / \partial E, \quad \tilde{\omega}_{if} = \varepsilon_i(E) - \varepsilon_f(E)$$

is valid, firstly, for $\omega_{if} = \varepsilon_i(E) - \varepsilon_f(E - \omega)$. Secondly, the quantum quantities can be replaced by the corresponding classical quantities. The quantity $\tilde{\omega}_{if}(E)$ goes over into $n\omega_0(E)$, where $n = i - f$ is the number of the harmonic, while $\omega_0(E)$ is the frequency of the classical vibrations of a particle in the channel.

Let us now find the classical analog of the derivative $\partial \varepsilon_i / \partial E$ for channeled particles. According to the Bohr-Sommerfeld rule

$$\int_{x_1(\varepsilon)}^{x_2(\varepsilon)} [2E(\varepsilon_n - U(x))]^{1/2} dx = 2\pi(n + 1/2).$$

Let us differentiate this equality with respect to the parameter E . Since the integrand vanishes at the turning points x_1 and x_2 , the result will have the following form:

$$\frac{d\epsilon}{dE} \int_{x_1}^{x_2} \left[\frac{E}{\epsilon - U(x)} \right]^{1/2} dx = - \int_{x_1}^{x_2} [(\epsilon - U(x))/E]^{1/2} dx. \quad (16)$$

The integral on the right-hand side of (16) is proportional to the transverse kinetic energy, $\epsilon_{kin} = Fv_{\perp}^2/2$, averaged over the period of the classical motion, while the integral on the left-hand side is proportional to the period of the motion. Therefore, in the classical limit

$$\partial \epsilon_{kin} / \partial E = -\epsilon_{kin} / E$$

and the relation (15) assumes the form [see also (22) in Ref. 17]:

$$\omega = 2\pi\omega_0 / (E^{-2} + \theta^2 + 2(\epsilon_{kin}/E)). \quad (17)$$

On the other hand, from the requirement that the longitudinal momentum of the particle,

$$p_{\parallel} = v_{\parallel} / [1 - (v_{\parallel}^2 + v_{\perp}^2)]^{1/2},$$

be conserved in classical motion in the potential of the planes, we obtain for the longitudinal velocity in the ultrarelativistic limit ($E_{\parallel} \gg 1$, $v_{\perp}^2 \sim \epsilon/E \ll 1$) the expression

$$v_{\parallel} \approx 1 - (E^{-2} + v_{\perp}^2)/2. \quad (18)$$

Thus, the denominator in (17) can be represented in the form

$$E^{-2} + \theta^2 + 2(\epsilon_{kin}/E) \approx 2(1 - \bar{v}_{\parallel} \cos \theta),$$

where \bar{v}_{\parallel} is the particle's longitudinal velocity, (18), averaged over the period of the transverse vibrations. Therefore, the expression (15) correctly takes the Doppler effect into account in the classical limit, while the expression (14), obtained by Baryshevskii *et al.*¹⁵ is at variance with this relation because of the presence of the above-indicated additional, generally speaking fairly large terms in (14). It should also be noted that the experimental data (see Table I and Sec. 5 below) are in good agreement with the theoretical computation based on the relation (17).

3. ESTIMATE OF THE EFFECT OF THE VARIOUS FACTORS ON THE RADIATION SPECTRUM

The actual values (5) and (6) of the transition-current matrix elements in the general expression (1) for the spectral-angular distribution were obtained without allowance for the periodicity of the potential of the planes as a function of x . This corresponds to the fact that the quantum tunneling of the particles through the potential barrier between neighboring channels was neglected. In the case of high particle energies ($> 10-100$ MeV), which

TABLE I.

E , GeV	$\lambda_{\omega_{max}}^{(1)}$ MeV [7]	$\lambda_{\omega_{max}}^{(1)}$ MeV (17)	E , GeV	$\lambda_{\omega_{max}}^{(1)}$ MeV [7]	$\lambda_{\omega_{max}}^{(1)}$ MeV (17)
2		12	10	90	86
4	23	30	14	120	121
6	42	49	16		137

is primarily of interest to us in the present paper, and in which the transverse motion is quasiclassical, this neglect is entirely justified. Since the tunneling probability turns out in this case to be exponentially small, its consideration does not lead to any appreciable effect.⁶ It is possible, however, that the transverse-energy level broadening connected with the leakage through the barrier plays a role at particle energies of the order of several MeV. In this case, however, it is also necessary to take into account the effect of the broadening due to the inelastic collisions of the channeled particles with the electrons and with the vibrating crystal atoms. It is significant that allowance for the tunneling in no way affects the general expression (1). It is only necessary that, in computing the basis wave functions, the boundary conditions requiring the vanishing of these functions and their derivatives, which enter in the transition current's matrix elements $I_{if}^{(1)}$ and $I_{if}^{(2)}$, be replaced by the more general conditions

$$\psi(x+d) = e^{i\kappa d} \psi(x), \quad \psi'(x+d) = e^{i\kappa d} \psi'(x), \quad (19)$$

which are a consequence of the Floquet-Bloch theorem (see, for example, Ref. 19). In the relations (19), d is the period of the planar potential and κ is a quantum number (quasimomentum) characterizing the state of the transverse motion: the eigenstate of the Hamiltonian for the transverse motion is now characterized by this number as well as by level (band) number.

The initial and final states in the expressions for the current's matrix elements in (1) do not necessarily belong to the discrete energy spectrum. In its general form, the expression (1) also describes the emission in the case of quasichanneling, when the initial and final states of the transverse motion belong to the continuous spectrum, as well as the emission occurring in transitions from the continuous into the discrete spectrum, i.e., from the state of quasichanneling into that of channeling.

Let us estimate the intensity and frequency distribution of these types of radiation for the case of high particle energies. The transverse motion is quasiclassical, starting roughly from energies $\sim 10^7$ eV for positrons and 10^8 eV for electrons. As a result, we obtain for the transition current's matrix elements, computed by the stationary-phase method with the aid of the quasiclassical wave functions, the following estimate [see, for example, (51.6) in Ref. 20]:

$$I_{if}^{(2)} \sim \exp[-(\Phi(\epsilon_i, E_i) - \Phi(\epsilon_f, E_f))], \quad I_{if}^{(1)} \sim \frac{\epsilon_i}{E} I_{if}^{(2)},$$

where

$$\Phi(\epsilon, E) = \text{Im} \int_a^{\infty} [2E(\epsilon - U(x))]^{1/2} dx,$$

and the integration is performed from the point, a , in the upper half-plane of the variable x where $U(a) = \epsilon$ to the singular point of the potential nearest to the real axis. Choosing the potential on the form $U(x) = -U_0 \times \cosh^{-2}(x/b)$, we easily find that

$$\Phi(\epsilon) = b(2E)^{1/2} \left(\frac{U_0^{1/2}}{2} \ln \frac{8U_0}{3U_0 + \epsilon} + \epsilon^{1/2} \arcsin \left(\frac{\epsilon}{\epsilon + U_0} \right)^{1/2} \right), \quad \epsilon > 0;$$

$$\Phi(\epsilon) = b(2E)^{1/2} \left(\frac{U_0^{1/2}}{2} \ln \frac{8U_0}{3U_0 + \epsilon} + |\epsilon|^{1/2} \text{Arcsin} \left(\frac{|\epsilon|}{\epsilon + U_0} \right)^{1/2} \right), \quad \epsilon < 0.$$

From this it follows that the matrix elements for transitions between states whose energy difference, $\varepsilon_i - \varepsilon_f$, is comparable to the depth, U_0 , of the potential contain the exponentially small factor⁴⁾ e^{-p} , where $p \sim b/\lambda_0$ —the quasiclassicality parameter—is the ratio of the width of the well to the de-Broglie wavelength, $\lambda_0 \sim (2EU_0)^{-1/2}$, for the transverse motion (the number of discrete levels in the well). Therefore, the maximum spectral density of the intensity of the radiation emitted in transitions from the continuous transverse-energy spectrum into the discrete spectrum turns out on the average (with respect to ε within the limits from zero to U_0) to be negligibly small in comparison with the analogous quantity for the radiation in the cases of channeling and quasichanneling. For the last two types of radiation there always exists a transverse-energy region, $\varepsilon_f \approx \varepsilon_i - \omega_0$ (where ω_0 is the frequency of the classical motion), in which the phase difference $\Phi(\varepsilon_i, E_i) - \Phi(\varepsilon_f, E_f)$ is small and the transition matrix elements reduce to the Fourier transforms of the corresponding classical quantities [see (9) in Ref. 7]. At the same time, the probability for radiative transitions from the continuous into the discrete spectrum, when on the average $\varepsilon_i - \varepsilon_f \sim \varepsilon_i$, vanishes in the classical limit. With transverse energies $\varepsilon \sim U_0$, the characteristic radiation frequencies for the cases of channeling and quasichanneling coincide in order of magnitude, while the characteristic radiation frequencies for the transition from the state of quasichanneling into that of channeling turn out on the average to be higher by roughly a factor of $p \gg 1$.

Results of actual radiation-spectrum computations, carried out in the classical limit, for the case of quasichanneling of positrons in a parabolic potential between the planes are presented in Ref. 7. This type of emission plays, together with the emission in the case of channeling, a definite role (see below) in the cases in which a fairly large fraction of the particles is not trapped in the channel, or is ejected from it as a result of the inelastic scattering processes.

In contrast, the emission occurring in the transition from the state of quasichanneling into the state of channeling at fairly high particle energies is unimportant. Therefore, the conclusions drawn by Kalashnikov *et al.*²¹⁻²³ that, for electrons of high energies (of the order of several GeV) entering, moreover, the crystal in a direction parallel to a crystallographic plane, the dominant role is played by the emission occurring in transitions from the continuous into the discrete spectrum when the population of the continuous-spectrum states is negligibly small are totally untenable (for more details see Sec. 5 below).

Let us now estimate the effect of the finiteness of the mean free path of the particles in the channeling regime on the radiation spectrum. For this purpose, let us introduce the radiation coherence length, which is defined in the same way as in the case of bremsstrahlung^{24,25}:

$$l_{\text{coh}} = \lambda / (1 - v_{\parallel} \cos \theta).$$

Taking into account the relations, (15) and (17), between the radiation frequency and the angle of emission by channeled particles, we find that the coherence length for the emission at the fundamental frequency coin-

cides with the wavelength of the particle oscillations in the channel for any frequency (and emission angle), i. e., $l_{\text{coh}} = l_{\text{osc}} \equiv 2\pi/\omega_0$. If, on the other hand, the maximum angle of deflection of the particles by the field becomes greater than the effective emission angle and the requirement that the radiation be of a dipole nature is not met, then the maximum of the spectral distribution of the radiation shifts toward the region of higher harmonics ($n > 1$), for which $l_{\text{coh}} = l_{\text{osc}}/n$.

A finite mean free path of a particle in the channeling regime can significantly affect the spectral distribution of the radiation only in the case in which the coherence length exceeds the mean free path. This case is, however, not realized in the channeling regime. In fact, there exists a region of longitudinal distances of the order of $l_{\text{osc}}/4$ near the crystal boundary where the free transverse particle motion changes into finite motion.^{26,35} In this region the particle states are described by a superposition of the stationary wave functions, ψ_n , of the transverse motion. The phase relations between the different ψ_n become unimportant and the channeling process can be considered to have attained the steady state only at distances significantly greater than l_{osc} . Therefore, the description of the channeling and the emission process in terms of discrete states (periodic trajectories) presupposes that the mean free paths are significantly greater than l_{osc} .

Another aspect of the boundary effect consists in the appearance of fairly hard transition radiation.²⁷ It is, however, significant that this radiation does not interfere with the radiation emitted in the channeling regime and can be considered independently. This can be seen from the following estimates. The transition radiation is substantial right up to frequencies $\omega_{\text{tr}} \sim \omega_p \gamma$, where ω_p is the plasma frequency of the electrons of the medium,²⁷ while the characteristic radiation frequencies for the case of channeling, which correspond to $\theta \sim 1/E$, are $\omega_{\text{ch}} \sim \omega_0 E^2$. A concrete calculation shows that ω_{ch} significantly exceeds ω_{tr} , starting from particle energies of the order of several MeV, and therefore their interference can be neglected. True, a channeled particle can emit frequencies significantly lower than ω_{ch} . But such frequencies are emitted at angles $\theta \gg 1/E$ [see (17)], and therefore the interference with the transition radiation, which is directed at angles $\theta \leq 1/E$, also turns out to be significant (γ is the Lorentz factor).

4. COMPUTATION OF THE AVERAGED POTENTIAL OF THE PLANES

To determine the averaged potential of the planes and of the axes, it is necessary to know the potential, $\varphi(r)$ of the individual atoms. Appleton *et al.*²⁸ have used the Moliere approximation⁵⁾ for the potential of the atom, and have obtained, with allowance for the isotropic thermal vibrations of the atoms, an analytic representation for the averaged potential of the plane.

It is well known²⁹ that under the condition⁶⁾ when $\varphi(r) > 10$ the Thomas-Fermi model describes the atomic potential sufficiently well. But for sufficiently small nuclear charges Z , or at sufficiently large distances

from the nucleus, the potential can deviate significantly from the Thomas-Fermi model.

The following equation was derived by Firsov²⁹ for the potential of an atom with nuclear charge $Z > 3$ on the basis of the statistical theory of the atom:

$$\Delta\varphi = 1.2\varphi^{3/2} + 0.81\varphi. \quad (20)$$

The first term on the right-hand side of Eq. (20) is the Thomas-Fermi term; the second (of the order of $Z^{-2/3}$) takes the quantum exchange effects into account. As has been shown by Kompaneets and Pavlovskii,³⁰ allowance for the derivative correction,³¹ which is also proportional to $Z^{-2/3}$, has virtually no effect on the potential because of the small proportionality factor.

An approximate solution to Eq. (20) has been obtained by Firsov, and has the form

$$\varphi(r) = \frac{Z}{r} \frac{\text{sh}^2 \beta a}{\text{sh}^2 \beta (r+a)}, \quad \beta = 0.4 Z^{-1/3}, \quad a = 1.8. \quad (21)$$

The screening function for the Firsov potential [see (21)] for $Z = 18$ agrees within 3% with the screening function computed by the Hartree-Fock method, and with the Thomas-Fermi-Dirac screening function, which have been tabulated for different Z values (see, for example, Ref. 32). At the same time, the Firsov potential (27) for carbon differs markedly from the Thomas-Fermi and Molière potentials.

The averaged potential of a plane, computed with the aid of (21) without allowance for the thermal vibrations, has the form (in ordinary units)

$$U_{\text{av}}(x') = \frac{4\pi Z e^2 a_{TF}}{A_s \beta} \frac{\text{sh}^2 \beta a}{\exp[2\beta(a+x'/a_{TF})] - 1}, \quad (22)$$

where x' is the distance from the plane, $a_{TF} = 0.885 (\hbar^2/mc^2) Z^{-1/3}$, d_p is the interplanar spacing, and A_s is the area per atom of the plane.

The dashed curve in Fig. 1 shows the potential of the (110)-plane channel of diamond as computed with the aid of the formula (22). The dot-dash curve in the same figure represents the potential based on the calculations of Appleton *et al.*²⁸ The continuous curve is a plot of

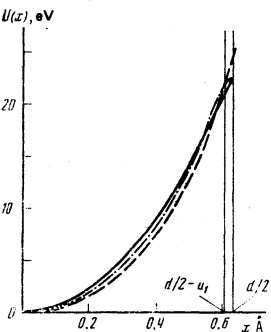


FIG. 1. Various approximations for the potential of the (110) planar channel in diamond. The dot-dash curve corresponds to the Molière model for the atom and takes the thermal vibrations into account, the dashed curve corresponds to the Firsov model for the atom, and the continuous curve is a plot of the parabola $U_0(x) = 4U_0x^2/d^2$ with the parameters $U_0 = 23$ eV, $d = 1.26$ Å.

the parabola $U(x) = 4U_0x^2/d^2$ with $U_0 = 23$ eV and $d = 1.26$ Å. It can be seen that the three curves do not differ greatly in the channel region. This indicates first and foremost that the averaged potential turns out in the present case to be less sensitive than the atomic potential to the various types of effects discussed above. Secondly, the parabola is a sufficiently good approximation to the potential everywhere except in the region of distances from the planes of the order of the amplitude u_1 of the thermal vibrations of the atoms. This region is comparatively narrow because of the high Debye temperature for diamond.

5. COMPUTATION OF THE SPECTRAL DISTRIBUTION OF THE RADIATION

In computing the radiation spectra in the $\omega \ll E$ region for positrons with energies 4–14 GeV in the case of channeling in diamond by the {110} planes, we proceeded from the formulas (1), (12), and (13). This corresponds to a transition to the classical description of both the emission process and the positron motion itself. The possibility of the latter is connected with the fairly large number of levels (~ 100 for 4 GeV) in the potential well of the transverse positron motion. Moreover, the transverse-energy levels turn out to be almost equidistant. Therefore, the transverse energy's discreteness, which could, in the case when the levels are highly nonequidistant and the resolving power of the photon spectrometer is fairly high, appear in the radiation spectrum even when there are a large number of levels, turns out from this point of view to be also insignificant.

After the integration with respect to the polar angle which is elementary because of the presence in (1) of the δ function, the spectral energy density of the radiation emitted by channeled positrons along a unit path assumes the form

$$\frac{d^2W}{d\omega dt} = I_0 \sum_{n=1}^{\infty} \frac{n}{1-\Omega^{(n)}} \sum_{m=-\infty}^{\infty} \sum_{m'=-\infty}^{\infty} (-1)^{m+m'} J_m(\beta) J_{m'}(\beta) \times [F_{mm'}^{(n)}(\gamma) + G_{mm'}^{(n)}(\gamma)] \eta(1-\Omega^{(n)}), \quad (23)$$

where

$$I_0 = \frac{e^2 \omega_0}{\pi}, \quad \beta = \frac{\omega \epsilon}{4\omega_0 E}, \quad \Omega^{(n)} = \frac{\omega}{\omega_{\max}^{(n)}},$$

$$\omega_{\max}^{(n)} = n \frac{2\omega_0 E^2}{1+\epsilon E}, \quad \omega_0 = \frac{1}{d} \left(\frac{8U_0}{E} \right)^{1/2}, \quad \gamma = 4[n\beta(1-\Omega^{(n)})]^{1/2}, \quad (24)$$

$$F_{mm'}^{(n)}(\gamma) = \left(1 - \frac{2m}{n}\right) \left(1 - \frac{2m'}{n}\right) \int_0^1 J_{n-2m}(\gamma x) J_{n-2m'}(\gamma x) \frac{(1-x^2)^{n/2}}{x^2} dx,$$

$$G_{mm'}^{(n)}(\gamma) = \left(1 - 2\Omega^{(n)} + \frac{2m}{n}\right) \left(1 - 2\Omega^{(n)} + \frac{2m'}{n}\right) \int_0^1 J_{n-2m}(\gamma x) \times J_{n-2m'}(\gamma x) \frac{dx}{(1-x^2)^{n/2}}$$

J_n is a Bessel function, η is the Heaviside unit function, and $x = \cos\varphi$. The parameters U_0 and d of the potential have been computed in Sec. (4) (see also Fig. 1).

We integrate over the azimuthal angle by the following method. We represent the Bessel-function product in the form of a series in powers of x (see, for example,

Sec. 7.2.7 in Ref. 10) and then integrate each term of the series. As a result, we can represent the functions $F_{mm'}^{(n)}(\gamma)$ and $G_{mm'}^{(n)}(\gamma)$ in the form of fairly rapidly converging series in the parameter γ :

$$F_{mm'}^{(n)}(\gamma) = \frac{(n-2m)(n-2m')}{n^2} \sum_{k=0}^{\infty} \frac{(-1)^k}{4k!} \gamma^{2k} \times \frac{\Gamma(l+1/2)\Gamma(l-1/2)(-1)^{n\eta((2m-n)(n-2m'))}}{\Gamma(|n-2m'|+k+1)\Gamma(|n-2m|+k+1)\Gamma(|n-2m|+|n-2m'|+k+1)}$$

$$G_{mm'}^{(n)}(\gamma) = \left(1-2\Omega^{(n)} + \frac{2m}{n}\right) \left(1-2\Omega^{(n)} + \frac{2m'}{n}\right) \sum_{k=0}^{\infty} \frac{(-1)^k}{2k!} \gamma^{2k} \times \frac{[\Gamma(l+1/2)]^2 (-1)^{n\eta((2m-n)(n-2m'))}}{\Gamma(|n-2m'|+k+1)\Gamma(|n-2m|+k+1)\Gamma(|n-2m|+|n-2m'|+k+1)}$$

$$l = 1/2(|n-2m|+|n-2m'|)+1.$$

The spectral distribution (23), of the radiation intensity was then averaged over the positron transverse energy ε . The transverse-energy distribution function $f(\varepsilon, t)$ depends, generally speaking, on the depth of penetration, t , of the particles into the crystal. Its initial value, $f(\varepsilon, 0)$, at the entrance crystal surface is determined in the general case by the condition³³

$$\varepsilon = E\theta_0^2/2 + U(x_0),$$

where x_0 is the transverse coordinate of the point where the particle enters the crystal and θ_0 is the angle of incidence with respect to the planes. Assuming that x_0 is a random quantity uniformly distributed within the limits of the channel, we easily find in the case of a parabolic potential that

$$f(\varepsilon, 0) = 1/2(\varepsilon - (\theta_0/\theta_L)^2 U_0)^{1/2} U_0^{1/2} \quad (25)$$

in the range $U_0(\theta_0/\theta_L)^2 < \varepsilon < U_0[1 + (\theta_0/\theta_L)^2]$, where $\theta_L = (2U_0/E)^{1/2}$ is the critical angle, and $f(\varepsilon, 0) = 0$ outside this interval.

The evolution of the particle transverse-energy distribution $f(\varepsilon, t)$ with increasing penetration depth is determined by the Fokker-Planck type of equation obtained earlier for the case of planar channeling of nonrelativistic protons.³⁴ This equation describes the multiple scattering of the channeled particles by the individual electrons of the crystal and the individual nuclei of the crystal lattice, which undergo random displacements from the equilibrium positrons as a result of thermal vibrations. Since only the assumption that the multiple-scattering angles are small is made in the derivation of this equation, it has the same general form in the cases of relativistic and heavy nonrelativistic particles:

$$\frac{\partial f(\varepsilon, t)}{\partial t} = \frac{\partial}{\partial \varepsilon} \left(\frac{1}{2} \left\langle \frac{\Delta \varepsilon^2}{\Delta t} \right\rangle T \frac{\partial f(\varepsilon, t)}{\partial \varepsilon} \right), \quad (26)$$

where $T = T(\varepsilon)$ is the vibration period of the particles in the channel, $\langle \Delta \varepsilon^2 / \Delta t \rangle$ is the mean square transverse-energy change averaged over the particle-vibration period. This change can be expressed in terms of the mean squared multiple-scattering angle, $\Delta \theta^2 / \Delta t$, by the relations

$$\langle \Delta \varepsilon^2 / \Delta t \rangle = 4 \langle (\Delta \varepsilon / \Delta t) (\varepsilon - U(x)) \rangle, \quad (27)$$

$$\langle \Delta \varepsilon / \Delta t \rangle = [(1+E)/2] \langle \Delta \theta^2 / \Delta t \rangle.$$

Here, in contrast to the nonrelativistic case,³⁴ the re-

lativistic increase of the particle mass is taken into account in the last relation. The angle brackets in (26) and (27) indicate averaging over the period of the particle motion:

$$\langle F(x) \rangle = \left(\frac{2}{E} \right)^{1/2} \int_0^{x_m(\varepsilon)} \frac{F(x) dx}{(\varepsilon - U(x))^{1/2}} \frac{1}{T(\varepsilon)}, \quad (28)$$

where $x_m(\varepsilon)$ is the maximum deviation of a particle from the center of the channel. For channeled positrons, $x_m(\varepsilon)$ is determined by the turning point in the transverse motion, while for above-the-barrier positrons x_m does not depend on the transverse energy ε , and is equal to half the distance between the central planes.

It should be borne in mind that it becomes clearly necessary to use in place of (26) the quantum kinetic equations for the level populations in the light-relativistic-particle case, in which the number of transverse-energy levels is not large. Such equations have been obtained for nonrelativistic protons.³⁵ But the quantum effects in the latter case are not so important. They also turn out to be insignificant in the case of positrons with energies of several GeV, since the number of transverse-energy levels for positrons with such energies is, as a result of the relativistic increase of the mass, of the same order of magnitude as the number of levels for the nonrelativistic proton. For electrons the quantum effects in the case of planar channeling may turn out to be important even at energies of about 1 GeV, since for them the potential well is narrower and the number of levels is smaller than the number for positrons by a considerable factor (see Fig. 1 in Ref. 7).

As has already been noted above, in a perfect crystal the mean change, $\Delta \varepsilon / \Delta t$, in the transverse particle energy is largely due to scattering by the electrons of the crystal and the vibrating nuclei:

$$\Delta \theta^2 / \Delta t = (\Delta \theta^2 / \Delta t)_e + (\Delta \theta^2 / \Delta t)_{in}.$$

In computing the contribution from the scattering by the nuclei, we used the following form of $(\Delta \theta^2 / \Delta t)_{in}$ (Ref. 36):

$$(\Delta \theta^2 / \Delta t)_{in} = (\Delta \theta^2 / \Delta t)_a P_n(x), \quad (29)$$

where $(\Delta \theta^2 / \Delta t)_a$ is the mean square angled of multiple scattering by atoms in an amorphous material, while

$$P_n(x) = \frac{d}{u_1 (2\pi)^{1/2}} \exp\left(-\frac{x^2}{2u_1^2}\right)$$

is the probability distribution for the displacements of the nuclei of the crystal lattice from the atomic plane, u_1 being the amplitude of the thermal vibrations of the nuclei. The mean squared multiple-scattering angle in an amorphous target is, as is well known, equal to

$$(\Delta \theta^2 / \Delta t)_a = E_e^2 / E^2 L,$$

where $E_e = 21$ MeV and L is the radiation length.

The contribution from the scattering by the electrons was computed in the following manner. The transverse energy change occurring in the scattering by the electrons was expressed in terms of the total positron-energy losses due to the near collisions by the relation^{33,37}

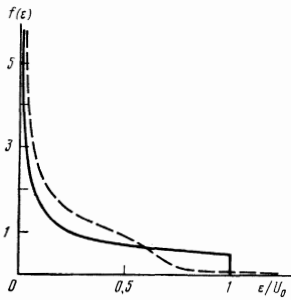


FIG. 2. The transverse-energy distribution function for the particles in the channel. The continuous curve depicts the initial distribution; the dashed curve, the distribution as averaged over a thickness of $80 \mu\text{m}$. The area under the curve is proportional to the number of particles in the channel.

$$\left(\frac{\Delta \varepsilon}{\Delta t}\right)_e = \frac{1}{E} \left(\frac{dE}{dt}\right)_{e_i}$$

With allowance for the Fermi-density effect and the equipartition rule for energy losses due to near and distant collisions, the positron-energy losses by near collisions have the form (see, for example, Ref. 38)

$$\left(\frac{\Delta E}{\Delta t}\right)_{e_i} = 2\pi e^4 n \left(\ln \frac{(2E)^{1/2}}{\omega_p} - \frac{11}{24} \right),$$

where ω_p is the plasma frequency of the medium and $n = n(x)$ is the electron density, which depends on the distance to the atomic plane. According to the Poisson equation, the form of this dependence is given by the relation

$$n(x) = \frac{1}{4\pi e} \frac{d^2 U}{dx^2},$$

where $U(x)$ is the potential depicted in Fig. 1 by the dot-dash curve.

The period $T(\varepsilon)$ of the channeled-positron motion does not, in the parabolic-potential approximation, depend on the transverse energy $T_0(\varepsilon) = \pi d(E/2U_0)^{1/2}$. The period of the motion of the above-the-barrier ($\varepsilon > U_0$) positrons is given in this model by the relation

$$T_{ab}(\varepsilon) = d \left(\frac{E}{2U_0} \right)^{1/2} \arcsin \left(\frac{U_0}{\varepsilon} \right)^{1/2}.$$

Figure 2 shows the initial transverse-energy distribution function, as well as the depth-averaged distribution function obtained as the result of the numerical solution of Eq. (26) for the case of entry of 6-GeV positrons parallel to the $\{110\}$ planes of a diamond single crystal of thickness $80 \mu\text{m}$. A comparison of these curves shows that the transverse-energy distribution function varies fairly slowly, except in the region of transverse energies higher than the value $0.7U_0$, which roughly corresponds to the critical Lindhard angle. Although the total number of channeled particles decreases insignificantly in the process (by roughly 20%), as a detailed calculation shows, the dechanneling affects the radiation intensity, since the particles with high transverse energies (and, consequently, large vibration amplitudes) make a significant contribution to the radiation.

The results of the computation of the radiation spectra

in a diamond crystal of thickness $80 \mu\text{m}$ are illustrated by Table I and the series of graphs. The averaging over ε was carried out with the initial distribution function, which takes account of only the angular spread of the incident beam, and the depth-averaged function.

Table I shows the dependence of the maximum photon energy, $\hbar\omega_{\text{max}}^{(1)}$, of the first harmonic [see (24)] on the positron energy E in the case of channeling by the $\{110\}$ planes of diamond ($U_0 = 22 \text{ eV}$, $d = 1.26 \times 10^{-8} \text{ cm}$). In constructing Table I we set the transverse energy equal to the barrier height (i.e., we set $\varepsilon = U_0$) in the formula (17). This choice is justified by the fact that the positrons with this transverse energy make the greatest contribution to the intensity in the region of the peak of the distribution. This is also corroborated by further numerical emission-spectrum calculations. Table I also shows the experimental data.⁹ Thus, the theoretical and measured values of $\hbar\omega_{\text{max}}^{(1)}$ are in fairly good agreement, but only when allowance is made for the parametric coupling of the longitudinal and transverse motions [i.e., for the term εE in the denominator of (24)]. Therefore, it may be concluded that this effect^{6,8} has been experimentally observed.

The continuous curves in Fig. 3 show the results of a detailed computation, for 4-, 6-, 10-, and 14-GeV positrons, of the spectral distribution of the radiation energy per unit path length in an $80\text{-}\mu\text{m}$ -thick diamond crystal in the case in which the $\{110\}$ planes are oriented parallel to the incident beam having an angular spread of $\Delta\theta = 10^{-5}$. The dashed curves indicate the contribution of the individual harmonics to the total intensity, and the dot-dash curves show the results of the computation of the same spectrum with the particles' depth-averaged ε distribution, which takes account of the dechanneling. Notice that the latter curves are plotted in absolute values, while the continuous and dashed curves are multiplied, for convenience of comparison, by the factor K indicated in the figure. The points on the graphs represent the experimental values obtained by Miroshnichenko *et al.*⁹ in the case of an $80\text{-}\mu\text{m}$ -thick target. It should be noted that in the indicated experiments the photons were registered by a Cerenkov total-absorption shower spectrometer. Such a spectrometer registers only the total electromagnetic-radiation energy produced during the passage of a positron through the crystal. Therefore, the spectra presented in Ref. 9 are in fact the photon-emission spectra only if the probability for the emission of two or more photons with a given (within the limits of the resolution of the spectrometer) total energy is significantly lower than the probability for the emission of a single photon with the same energy. As estimates based on the theoretical spectra presented in Fig. 3 show, this condition was satisfied for the target of thickness $80 \mu\text{m}$, and clearly violated for the $600\text{-}\mu\text{m}$ target, used in the experiments described in Ref. 9. Therefore, it is possible to compare directly the computed radiation spectra only with the results obtained for the $80\text{-}\mu\text{m}$ thick target. As to the results obtained for the $600\text{-}\mu\text{m}$ -thick target, further calculations taking the multiplicity of the photon emission in the target into account are required here.

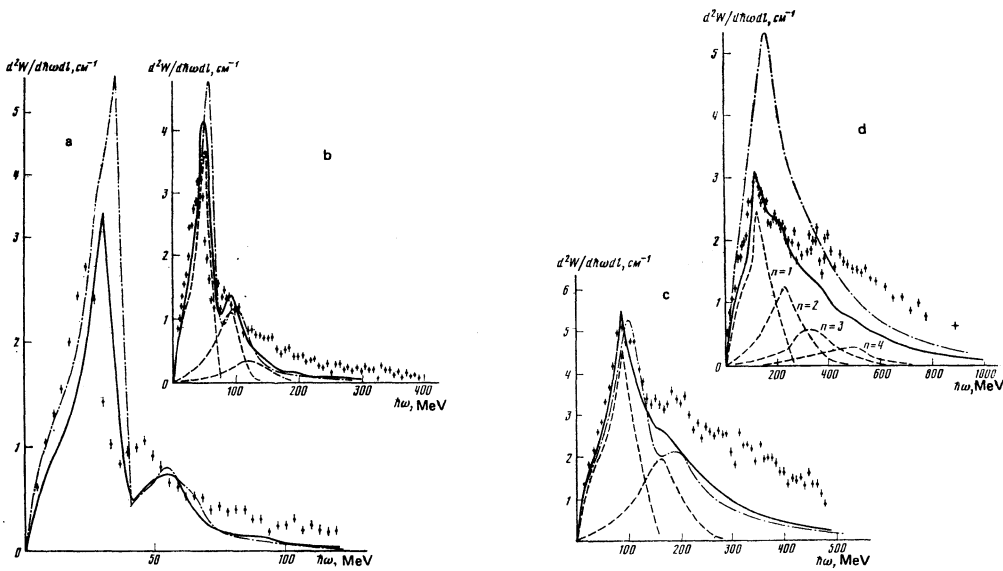


FIG. 3. Spectral distribution of the energy of the radiation emitted by positrons along a unit path in the case of channeling in an 80- μm -thick diamond crystal along the $\{110\}$ planes. The dot-dash curve represents the case of averaging over ϵ with the depth-averaged distribution function, which takes account of the dechanneling, while the solid curve is for the case averaging over ϵ with the distribution function that takes only the initial 10^{-5} -rad angular spread of the beam into account. The theoretical values shown by the solid curve have been decreased by a factor of K in the graphs: a) the positron energy $E = 4$ GeV, $K = 2.5$; b) $E = 6$ GeV, $K = 2$; c) $E = 10$ GeV, $K = 1.5$; d) $E = 14$ GeV, $K = 2.5$; the dashed curves show the contributions of the individual harmonics.

According to the theoretical calculations, the contribution of the higher harmonics increases with increasing positron energy (see also Sec. 4 of Ref. 6). Also taken into consideration is the variation of $\hbar\omega_{\text{max}}^{(n)}$ [see (24)] when the transverse energy is varied from zero to U_0 , which leads to effective broadening of the spectrum in the region of the peak. These characteristics of the spectra have been experimentally observed. The small shift in position of the peaks is apparently due to an error in the theoretical value of the planar potential $U(x)$, or to an error in the calibration of the spectrometer.

The discrepancy between the absolute theoretical and experimental intensity values (see Fig. 3) has a double character: in the region of the principal peak (of the first harmonic) the theoretical values exceed (except in the 10-GeV case) the experimental values, while the opposite is the case in the region of the higher harmonic. The decrease of the intensity in the region of the principal peak is apparently explained by additional dechanneling of the particles as a result of the imperfection of the crystal (the presence of a mosaic structure, dislocations). The dechanneling leads to a general decrease in the radiation intensity as a result of the ejection of particles from the channel, and it can be effectively taken into account, as can be seen from Fig. 3, by dividing the theoretical results by some coefficients. On the other hand, the dechanneled particles should, as shown below, make a contribution to the emission at the frequencies of the second and higher harmonics; this contribution was not taken into consideration in the computation of the curves shown in Fig. 3.

As a calculation for the parabolic potential shows, in the course of the periodic collisions with the crystal planes, the particles with energy $\epsilon > U_0$ radiate at the characteristic frequencies

$$\omega_{\text{max}}^{(n)} = n \cdot 2^{1/2} \pi U_0^{1/2} E^{3/2} d^{-1} [(1 + \epsilon E) \xi + E(U_0(\epsilon - U_0))^{1/2} - 2U_0 E \xi^{-1}]^{-1}, \quad (30)$$

$$n = 1, 2, 3, \dots, \quad \xi = \arcsin(U_0/\epsilon)^{1/2}.$$

These frequencies are determined by the time of flight of the positrons between neighboring planes and by the Doppler effect, and depend on the transverse energy ϵ even at low energies ($\epsilon E \ll 1$), in contrast to the case of channeled particles (24).

It is significant that the characteristic frequencies of the radiation emitted by above-the-barrier particles (i. e., those with $\epsilon > U_0$) are at least double the corresponding frequencies for channeled particles [cf. (24) and (30)]. Therefore, in the case under consideration the above-the-barrier particles should make the dominant contribution to the frequency region roughly equal to the region of the second harmonic of the channeled frequencies. It is therefore clear that the remaining (after the normalization of the theoretical curves) deviation from the experimental values of the spectral density can be compensated for if the contribution of the above-the-barrier particles is taken into consideration. From this it also follows that the principal peak in the measured spectra is definitely due to the emission from the channeled positrons. Let us note, for comparison that in the case of electrons the channeled particles and the above-the-barrier particles with transverse energies close to the barrier height radiate at roughly the equal characteristic frequencies (see Fig. 4). Therefore, without an additional analysis of the electrons with respect to their angles of emergence from the crystal, it is difficult to say with certainty that the observed peak in the spectrum³⁹ is due to the emission of only the channeled electrons.

The necessary formulas for the computation of the contribution made by the above-the-barrier particles

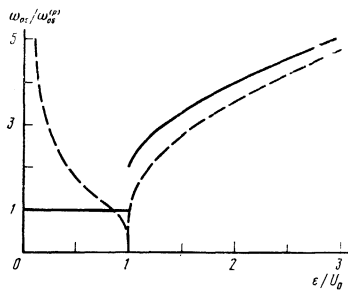


FIG. 4. Dependence of the frequencies ω_{0s} of the transverse motion of the electrons and positrons on their transverse energy for the model potential having the shape of a parabola between neighboring planes. The quantity (ϵ/U_0) is the abscissa, and the ordinates are the frequencies of the motion in units of the vibration frequency of the channeled positrons, $\omega_{0s}^0 = (1/d)(8U_0/E)^{1/2}$. The solid curve pertains to positrons; the dashed curve, to electrons. At high transverse energies all the curves approach the dependence $d^{-1}(2\epsilon/E)^{1/2}$, which corresponds to almost straight-line trajectories.

to the radiation intensity are derived in Ref. 7. Unfortunately, the distribution of the positrons over the angles of emergence from the crystal has not been experimentally analyzed. The lack of this information makes it impossible for us to carry out an exact spectrum calculation for the radiation from the above-the-barrier particles, since the form of the spectrum significantly depends on their transverse-energy distribution function.

On the whole, the foregoing comparison of the theoretical predictions with the experimental data obtained by Miroshnichenko *et al.*⁹ shows that the effect of intense radiation from high-energy channeled positrons in the continuous potential of planes has been experimentally observed. The experimental results confirm not only the relatively high radiation intensity predicted by theory,¹⁻⁸ but also many fine details of the radiation spectrum.

The authors express their gratitude to O. B. Firsov for his advice, which was useful in the computations of the planar potential, to R. O. Avakyan and I. I. Miroshnichenko for making their detailed experimental data available to us, and to E. P. Velikhov and V. M. Galitskii for their encouragement during the investigations and for a discussion of the results.

¹We use the system of units in which $\hbar = m = c = 1$.

²This result pertains only to the case of planar channeling. For axial channeling there is no dependence on Q , and the relation between the frequency and the polar angle of emission has the form $\omega/2[\theta^2 + 1/E(E - \omega)] = \omega_{if}$.

³The accuracy of such an approximation can be estimated with the aid of the equalities $J_0(\frac{1}{4}) \approx 0.98$ and $J_1(\frac{1}{4}) \approx 0.12$.

⁴This result remains valid for any other realistic choice of a model potential.

⁵This potential is close to the Thomas-Fermi potential.

⁶In this section we use the atomic units.

¹M. A. Kumakhov, Dokl. Akad. Nauk SSSR 230, 1077 (1976) [Sov. Phys. Dokl. 21, 581 (1976)]; Phys. Lett. A57, 17 (1976).

- ²M. A. Kumakhov, Zh. Eksp. Teor. Fiz. 72, 1489 (1977) [Sov. Phys. JETP 45, 781 (1977)].
- ³M. A. Kumakhov and R. Wedell, Phys. Status Solidi B84, 581 (1977).
- ⁴V. A. Bazylev and N. K. Zhevago, Zh. Eksp. Teor. Fiz. 73, 1697 (1977) [Sov. Phys. JETP 46, 891 (1977)].
- ⁵V. V. Beloshitskiĭ and M. A. Kumakhov, Zh. Eksp. Teor. Fiz. 74, 1244 (1978) [Sov. Phys. JETP 47, 652 (1978)].
- ⁶N. K. Zhevago, Zh. Eksp. Teor. Fiz. 75, 1389 (1978) [Sov. Phys. JETP 48, 701 (1978)].
- ⁷V. A. Bazylev, V. I. Glebov, and N. K. Zhevago, Zh. Eksp. Teor. Fiz. 78, 62 (1980) [Sov. Phys. JETP 51, 31 (1980)].
- ⁸M. A. Kumakhov and Kh. Trikalinos, Zh. Eksp. Teor. Fiz. 78, 1623 (1980) [Sov. Phys. JETP 51, 815 (1980)]; Phys. Status Solidi B99, 449 (1980).
- ⁹I. I. Miroshnichenko, J. J. Murray, R. O. Avakyan, and T. Kh. Figut, Pis'ma Zh. Eksp. Teor. Fiz. 29, 786 (1979) [JETP Lett. 29, 722 (1979)].
- ¹⁰A. Erdelyi, ed. Higher Transcendental Functions, McGraw-Hill, New York, 1953 (Russ. Transl., Nauka, Moscow, 1973).
- ¹¹R. H. Pantell and M. J. Alguard, J. Appl. Phys. 50, 798 (1979).
- ¹²N. A. Korkhmazyan, Izv. Akad. Nauk Arm. SSR Ser. Fiz. 7, 114 (1972).
- ¹³D. F. Alferov, Yu. A. Bashmakov, and E. G. Bessonov, Zh. Eksp. Teor. Fiz. 63, 1226 (1973) [Sov. Phys. JETP 36, 646 (1973)].
- ¹⁴V. N. Baĭer, V. M. Katkov, and V. M. Strakhovenko, Preprint Inst. Yad. Fiz., Sib. Otd. Akad. Nauk SSSR, IYAF 80-03 (1980).
- ¹⁵V. G. Baryshevskii, I. Ia. Dubovskaya, and A. O. Grubich, Phys. Status Solidi B99, 205 (1980).
- ¹⁶V. G. Baryshevskii and I. Ia. Dubovskaya, Phys. Status Solidi B82, 403 (1977).
- ¹⁷V. G. Baryshevskii, A. O. Grubich, and I. Ia. Dubovskaya, Phys. Status Solidi B88, 351 (1978).
- ¹⁸R. Wedell, Phys. Status Solidi B99, 11 (1980).
- ¹⁹Neil W. Ashcraft and David N. Mermin, Solid State Physics, Holt, Rinehard, and Winston, 1976.
- ²⁰L. D. Landau and E. M. Lifshitz, Kvantovaya Mekhanika (Quantum Mechanics), Fizmatgiz, Moscow, 1963 (Eng. Transl., Addison-Wesley, Reading, Mass., 1965).
- ²¹É. A. Koptelov and N. P. Kalashnikov, Preprint Inst. Yad. Issled. Akad. Nauk SSSR, P-0054 (1977).
- ²²N. P. Kalashnikov and A. S. Ol'chak, Vzaĭmodeĭstviya yadernykh izlucheniĭ s monokristallami (Interaction of Nuclear Radiation with Single Crystals), MIFI, Moscow, 1979.
- ²³N. P. Kalashnikov, V. S. Remizovich, and M. I. Ryazanov, Stolknoveniya bystrykh zaryazhennykh chastits v tverdykh telakh (Collisions of Fast Charged Particles in Solids), Atomizdat, Moscow, 1980.
- ²⁴M. L. Ter-Mikaelyan, Zh. Eksp. Teor. Fiz. 25, 289, 296 (1953).
- ²⁵V. M. Galitskiĭ and I. I. Gurevich, Nuovo Cimento 32, 396 (1964).
- ²⁶Yu. Kagan and Yu. V. Kononets, Zh. Eksp. Teor. Fiz. 58, 226 (1970) [Sov. Phys. JETP 31, 124 (1970)].
- ²⁷G. M. Garibyan, Zh. Eksp. Teor. Fiz. 37, 527 (1959) [Sov. Phys. JETP 10, 372 (1960)].
- ²⁸B. R. Appleton, C. Erginsoy, and W. M. Gibson, Phys. Rev. 161, 330 (1967).
- ²⁹O. B. Firsov, Tezisy dokladov na 6-ĭ Vsesoyuznoĭ konferentsii po atomno-ĕlektronym (Abstracts of Papers Presented at the Sixth All-Union Conference on Atom-Electron Collisions), 1975, p. 146.
- ³⁰A. S. Kompaneets and E. S. Pavlovskii, Zh. Eksp. Teor. Fiz. 31, 427 (1956) [Sov. Phys. JETP 4, 326 (1957)].
- ³¹C. S. Weizsacker, Z. Phys. 96, 431 (1935).
- ³²P. Gambos, Die statistische Theorie des Atoms and ihere Anwendungen. Springer, Vienna, 1949.

- ³³J. Lindhard, *Mat. Fyz. Medd. Dan. Vid. Selsk.*, **34**, No. 14 (1965).
³⁴V. V. Beloshitskiĭ and M. A. Kumakhov, *Dokl. Akad. Nauk SSSR* **212**, 846 (1973) [*Sov. Phys. Dokl.* **18**, 652 (1973)]; *Fiz. Khim. Obrab. Mater.* **3**, 39 (1973).
³⁵Yu. Kagan and Yu. V. Kononets, *Zh. Eksp. Teor. Fiz.* **64**, 1042 (1973) [*Sov. Phys. JETP* **37**, 530 (1973)].
³⁶M. Kitagawa and Y. H. Ohtsuki, *Phys. Rev.* **B8**, 3117 (1973).
³⁷N. Bohr, *Penetration of Atomic Particles through Matter*,

- Danske Vid. Selsk. Mat.-fys. Medd.* **18**, 8 (1948) (Russ. Transl., Atomizdat, Moscow, 1970).
³⁸R. M. Sternheimer, *Phys. Rev.* **91**, 256 (1953).
³⁹A. O. Agan'yants, Yu. A. Vartanov, G. A. Vartapetyan, M. A. Kumakhov, Kh. Trikalinos, and V. Ya. Yaralov, *Pis'ma Zh. Eksp. Teor. Fiz.* **29**, 554 (1979) [*JETP Lett.* **29**, 505 (1979)].

Translated by A. K. Agyei

Interaction between electron-hole drops and dislocations in semiconductors

S. V. Bozhokin and D. A. Parshin

Leningrad Polytechnic Institute

(Submitted 20 May 1980; resubmitted 22 August 1980)
Zh. Eksp. Teor. Fiz. **80**, 627-637 (February 1981)

Elastic interaction between an electron-hole drop and a dislocation in a semiconductor is considered. It is shown within the framework of the isotropic model that the EHD interacts with an edge dislocation but not with a screw dislocation. The binding energy of the EHD with an edge dislocation is calculated and found to be three orders larger than the EHD-impurity binding energy. The trajectories of EHD in the elastic field of zero-initial velocity dislocation are calculated. Allowance for the EHD energy loss to emission of elastic waves and for friction against the lattice can cause the EHD to "fall" on the dislocation. It is shown that near the dislocation axis the EHD finds it more convenient to assume a cylindrical shape (to flow along the dislocation axis). If the semiconductor contains a network of dislocations, this flow of the electron-hole liquid (EHL) can lead to formation of a conducting cluster made up of EHL filaments.

PACS numbers: 61.70.Yq, 62.30.+d, 71.35.+z

1. It was shown by a number of experiments¹⁻³ that electron-hole drops (EHD) are localized in semiconductors on donor and acceptor impurities. For Ge samples with impurity density $n_i = 3 \times 10^{13} \text{ cm}^{-3}$ the force needed to detach the EHD from the impurity per electron-hole pair is approximately $f \sim 10^{-20} \text{ N}$ (for a drop radius of the order of 10^{-4} cm). This value agrees with a theoretical calculation of the EHD-donor binding energy.^{4,5} At lower densities, $n_i = 3 \times 10^{10} \text{ cm}^{-3}$, however, the dependence of the EHD detachment force on the drop radius turns out to be different than in the case of pinning of an EHD on an impurity,² thus pointing to the existence of other trapping centers. This is also attested to by the experimental data of Westervelt,² who notes that the coefficient of diffusion of an EHD in a Ge crystal with dislocations in an order of magnitude lower than in a crystal without dislocations. This is an indirect indication that dislocations can also serve as EHD trapping centers.

In the present study we have investigated the elastic interaction of an EHD with a dislocation, and determined the influence of this interaction on the pinning of the EHD. We show that the force needed to detach an EHD from an edge dislocation, per electron-hole pair, is inversely proportional to the square of the drop radius and, for example for a spherical drop of radius $a = 2 \times 10^{-4} \text{ cm}$, amounts to $4.8 \times 10^{-18} \text{ N}$. This exceeds by more than two orders the force needed to detach an

EHD from an impurity. The results is attributed to the fact that the radius of the electrostatic interaction of the EHD with the impurity is small and equals approximately the Debye screening radius r_d , whereas the elastic interaction of an EHD with a dislocation is not screened and the entire EHD volume interacts with the dislocation.

2. Consider a crystal with an isolated dislocation and containing an EHD. It is known that the EHD has elastic-stress fields⁶ and that the density of the crystal elastic energy, with allowance for the interaction of the EHD with the strain field, can be represented in the form^{7,8}

$$w = D_{ij} n(\mathbf{r}) u_{ij}(\mathbf{r}) + \frac{1}{2} c_{ijkl} u_{ij}(\mathbf{r}) u_{kl}(\mathbf{r}), \quad (1)$$

where $u_{ij}(\mathbf{r})$ is the strain tensor, D_{ij} is the combined strain potential of the electrons and hole, $n(\mathbf{r})$ is the coordinate-dependent density of the electrons and holes in the EHD, and c_{ijkl} are the elastic constants. Since the crystal contains two sources of elastic stresses, the strain tensor can be represented by the sum $u_{ij}(\mathbf{r}) = u_{ij}^e(\mathbf{r}) + u_{ij}^d(\mathbf{r})$, where $u_{ij}^e(\mathbf{r})$ is the strain tensor produced in the crystal by the EHD and $u_{ij}^d(\mathbf{r})$ is the strain tensor produced by the dislocation. The total elastic energy of the crystal $U = \int d\mathbf{r} w(\mathbf{r})$ consists of the drop's elastic energy U_e , of the dislocation elastic energy U_d , and of the energy U_{int} of the EHD interaction with the dislocation, for which the following expression